

## Numerical Estimation of $10^4$ Years Later Equilibrium Ice Sheet Profile in the Shirase Glacier Drainage Basin, East Antarctica

Shuji FUJITA<sup>1</sup>, Norikazu IKEDA<sup>1\*</sup>, Nobuhiko AZUMA<sup>2</sup>,  
Takeo HONDOH<sup>1</sup> and Shinji MAE<sup>1</sup>

数値計算による東南極白瀬氷河流域氷床の  $10^4$  年後の氷床平衡形の見積もり

藤田 秀二<sup>1</sup>・池田 範和<sup>1\*</sup>・東 信彦<sup>2</sup>・本堂 武夫<sup>1</sup>・前 晋爾<sup>1</sup>

**要旨:** 東南極, 白瀬氷河流域では, 近年の観測により氷床表面高度の低下が観測されている. この変動を氷床が近年の気候に適合していく過程としてとらえるならば, 現在の気候に対応する氷床の平衡形を求めれば, 現在の氷床の挙動を理解できる手がかりが得られる. 三次元非定常氷床流動モデルを用いて, 氷床の平衡形が見積もられた.

モデル計算には, 基盤地形, 表面涵養量, 氷床表面高度, 氷床表面温度について, 観測値とその外挿値を用いた. そして, 氷床表面温度, 表面涵養量, 地殻熱流量などのパラメーターを様々に変えた場合の氷床の形を求めた.

計算の結果, 計算を現在の氷床形から開始した場合  $10^4$  年後までの計算で氷床は平衡形に達した. 平衡形は, テストしたパラメーターに大きく依存するが, 一般的傾向としては氷厚は中流域で低下し下流域で増大する. やまと山脈近傍ではパラメーターの値を変えても氷床の変動は比較的小さいことが示された.

**Abstract:** Recent observations show that the ice sheet in the Shirase Glacier drainage basin, East Antarctica, is thinning. If the observed thinning is assumed to be a transitional process in which the ice sheet is adjusting to the present climate, an equilibrium ice sheet profile which adjusts to the present climate would provide us with information for understanding the present behavior of the ice sheet. The equilibrium ice sheet profile was estimated by using a three-dimensional non-steady state ice sheet model.

Estimations were carried out with data based on observations of bedrock topography, surface elevation, accumulation rate and surface temperatures, and their extrapolation for areas where there is no field data. And the equilibrium ice sheet profile against various parameters, e.g. surface temperatures, accumulation rate and geothermal heat flux, was investigated.

Results of the calculation showed that an almost stationary state of the ice sheet was achieved after  $10^4$  model years when started from the present profile of the ice sheet. The equilibrium ice sheet profile depended on bedrock topography and tested parameters sensitively, but the calculations indicated that ice-thickness tend to decrease in the middle-stream region in general. It was also revealed that the ice sheet in the vicinity of the Yamato Mountains was relatively stable even if the parameters were changed.

<sup>1</sup> 北海道大学工学部. Department of Applied Physics, Faculty of Engineering, Hokkaido University, Kita-13, Nishi-8, Kita-ku, Sapporo 060.

<sup>2</sup> 長岡技術科学大学機械系. Department of Mechanical Engineering, Nagaoka University of Technology, Kamitomioka-cho, Nagaoka 940-21.

\* 現, エスコリース(株). Esco Leasing Corporation, Nishi-11-4, Odori, Chuo-ku, Sapporo 060.

## 1. Introduction

The following observations and studies were carried out about the dynamical behavior of the ice sheet in the Shirase Glacier drainage basin (Fig. 1). NARUSE (1978, 1979) analyzed the result of triangulation chain survey which had been carried out in the area from the Yamato Mountains to Mizuho Plateau, which was in the middle-stream region of the Shirase Glacier drainage basin, along latitude 72°S. He investigated horizontal and vertical components of surface velocities and strain-rate at the surface. Taking into account the effect of the firn densification, he found that the ice sheet was thinning there by about 70 cm/a. With the result of observation by NARUSE, MAE (1979) estimated that velocity of 10 m/a within the horizontal surface velocity reported by NARUSE, which ranged between 13 and 21 m/a, was due to basal sliding. NISHIO *et al.* (1989) carried out observation of horizontal and vertical components of surface velocities along the flow line which was along longitude 39.5°E, and along 2000 m contour between Mizuho Station and the Belgica and the Yamato Mountains, by using the satellite doppler positioning system. They showed that the ice sheet is thinning in the region where ice elevation is lower than 2800 m. On the other hand, according to the result of radio echo-sounding on Mizuho Plateau, higher values of reflection intensity of radio echo than in the up-stream region were observed in the regions where the ice elevation was lower than 2500 m (OHMAE *et al.*, 1989; NISHIO *et al.*, 1989). This result suggests that the base is wet there.

Based on the above studies, it has been proposed that the recent thinning of the ice sheet in Mizuho Plateau is due to occurrence of basal sliding (MAE and NARUSE, 1978; NISHIO *et al.*, 1989) and decrease of the accumulation rate (MAE and NARUSE, 1978).

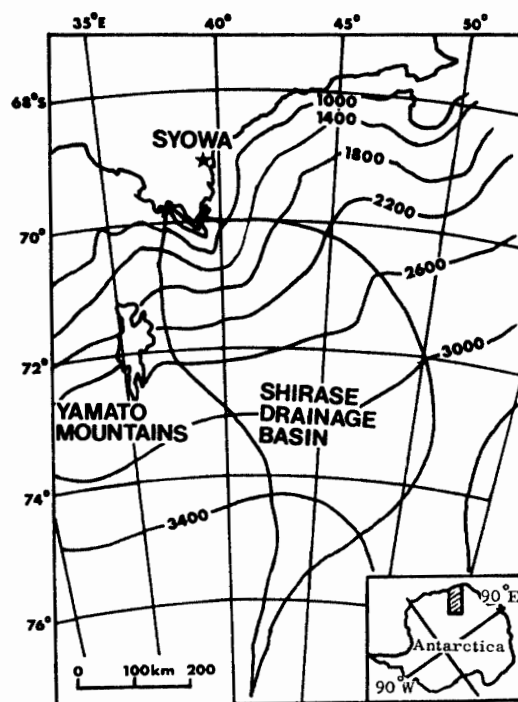


Fig. 1. Area map of the Shirase Glacier drainage basin.

If the observed thinning of the ice sheet is assumed to be a transitional process in which the ice sheet is adjusting to the present climate, an equilibrium ice sheet profile which adjusts to the parameters of the present climate would provide us with some information for understanding the recent thinning. In order to investigate the equilibrium ice sheet profile there, the three-dimensional non-steady state ice sheet model, which had been developed by NAGAO *et al.* (1982, 1984), was improved and used.

The numerical modeling of dynamical behavior of the ice sheet in the Shirase Glacier drainage basin was preliminarily made by NAGAO *et al.* (1984). The model, however, did not have a computational stability probably because of too coarse resolution of the grids into which the studied area was divided for calculation, or the unsuitable use of an explicit method to solve partial differential equations, or the lack of field data especially on the bedrock topography. Therefore, this model was improved first by employing the Finite Elements Method (FEM) and an implicit method to solve the partial differential equations. Next it was improved with the new data of bedrock elevation observed by the Japanese Antarctic Research Expedition (JARE) during the Glaciological Research Program in East Queen Maud Land. With these improvements, the model has acquired a computational stability, which enables us to investigate the equilibrium ice sheet profile against various parameters and discuss the instability of the ice sheet.

## 2. Outline of the Model and the Method for Calculating the Mass Flux

The model used in this study is an advance from the earlier three-dimensional modeling of NAGAO *et al.* (1984). Since the method for calculating mass flux of ice due to internal deformation has been described in NAGAO *et al.* (1982), this paper deals mainly with a method for calculating basal sliding and a particular improvement of the model.

The model developed by NAGAO *et al.* (1982) was an improvement of MAHAFFY's three-dimensional non-steady state ice sheet model (MAHAFFY, 1976), taking into account the temperature profile at a given place of the ice sheet, which was ignored in the previous case. MAHAFFY's model assumes that the flow is laminar, and ignores longitudinal stress and lateral shear stress. These assumptions are valid for a large ice sheet except near the terminus and up-stream of the mountains. One of the advantages of MAHAFFY's model is that arbitrary bed topography can be considered in it.

For saving the much of the computation task, NAGAO *et al.* (1982) proposed a simple method for calculating mass flux of ice. For the depth profile of the temperature at a given place, a linear profile is assumed which is formulated with the bottom temperature and the temperature gradient at the bottom. The bottom temperature can be derived by solving the equation of heat conduction including the horizontal advection term (RADOK *et al.*, 1970). The temperature dependence of the flow law of ice was converted from the Arrhenius equation to a simple expression. This conversion, together with the above assumption of temperature profile, made the calculation of mass flux very simple. NAGAO *et al.* (1982) estimated that the maximum error of mass flux caused by the assumption of linear temperature profile was less than 11%.

Basal sliding mechanism was also considered in the present study. This mech-

anism seems especially important in the Shirase Glacier drainage basin because it is considered to be one of the causes of the recent thinning of the ice sheet. WEETMAN (1957) proposed that regelation and enhancement of plastic flow around the bumps of the bedrock are the dominant mechanism of basal sliding. Although latter mechanism is not a linear function of basal shear stress, basal sliding velocity ( $u_b$ ) is assumed to be proportional to the basal shear stress and sliding is considered to occur in the area where the bottom of the ice sheet is at the pressure melting point of the ice in this study. Then  $u_b$  is expressed as,

$$u_b = -B_o \rho g H \left( \frac{dh}{dx} \right) f_s(T_b). \quad (1)$$

Here  $B_o$  is constant.  $\rho$  and  $g$  are the density of ice and gravitational acceleration, respectively.  $H$  is ice thickness and  $h$  is surface elevation. In the coordinate system,  $x$  is taken in the horizontal plane. Notation  $f_s(T_b)$  is given as

$$f_s(T_b) = \begin{cases} 0 & (\text{if } T_b < T_{mp}) \\ 1 & (\text{if } T_b = T_{mp}). \end{cases} \quad (2)$$

Here  $T_b$  and  $T_{mp}$  are bottom temperature and pressure melting point of ice, respectively.  $B_o$  was determined so that velocity due to basal sliding ranged between 50% and 75% of the surface velocity. This was based on estimation by MAE (1979) that velocity of about 10 m/a was due to the basal sliding in the surface velocity which ranged between 13 and 21 m/a measured by NARUSE (1978) along latitude 72° in MIZUHO Plateau.

One of particular techniques used in this study is Finite Elements Method (FEM). With this technique the area of the drainage basin was divided into a number of elements (Fig. 2) on which the mass flux of the ice is computed so as to satisfy the equation of mass continuity. Since in the down-stream region ice was expected to flow

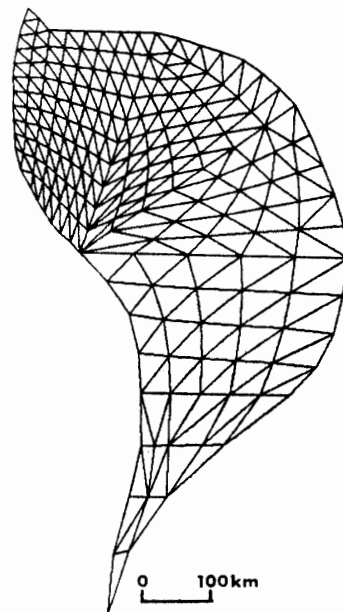


Fig. 2. Division of the studies area into finite elements.

relatively faster than the other regions, the ice sheet is represented with smaller elements. In this paper, the Shirase Glacier drainage basin is considered to be composed of three regions for convenient. They are defined as the up-stream region, the middle-stream region and the down-stream region. The boundary of these regions are latitude 74°S and 72°S. Another technique used in the model is an implicit method for solving partial differential equations. Equation of mass continuity is expressed with partial differential equation in this study. In general, the implicit solution provides computational stability in time-dependent simulations.

It should be noted that there are some limitations in the present model for estimating the dynamical behavior of the ice sheet. They are as follows. (1) Because longitudinal stress is ignored, this model is unrealistic at the terminus of the ice sheet. (2) Because the seaward boundary is fixed, advance of the ice sheet and effect of the ice shelf are not incorporated. (3) Steady state temperature profile is assumed. So the transitional state of temperature profile when the climate changes cannot be reconstructed. (4) Isostasy of the bed and change of the bedrock topography over a long period of time is not considered. (5) The outer margin of drainage basin is fixed.

Therefore the model in the present stage should be used for estimating dynamical behavior in the region except the ice sheet terminus and in a relatively short period of time, namely a situation where the drainage basin and the bed topography will not change significantly during that period. It seems proper to use this model for the objective of present study. For further applications the model should be improved.

### 3. Input Data and Boundary Conditions

The bedrock topography data were compiled into a contour map (Fig. 3) from the data published in NISHIO *et al.* (1984, 1986), FUJII *et al.* (1986), AGETA *et al.* (1987) and MAE and YOSHIDA (1987). For reading into computer, data were interpolated onto the place of nodes of finite elements. As for the regions where there is no field data, especially for the up-stream region, the values of the known regions were extrapolated. Initial elevation of the ice sheet surface (Fig. 1) has been obtained from the map "East Queen Maud Land-Enderby Land" that was edited by National Institute of Polar Research (Japan) in 1988.

For the accumulation rate, NAGAO (1982) expressed annual accumulation rate ( $A$ ) at a given place as a function of surface elevation and distance from the coast, as follows,

$$A = \text{bal}(h)/(1 + x/100). \quad (3)$$

Here  $x$  is distance from the coast to a given point expressed with km. Notation  $\text{bal}(h)$  is a function of elevation as in Fig. 4. It is based on compilation of surface mass balance data in the Shirase and the Sôya drainage basins made by YAMADA and WATANABE (1978), but adapted as a monotonously increasing function with  $h$ . We used eq. (3) for the surface mass balance in calculations. As the discharge of the ice sheet, instead of calving of ice-bergs at the terminus of the ice stream, the same amount of ablation is assumed to occur around the terminus.

Surface temperature ( $T_s$ ) is expressed as a function of elevation. It is based on

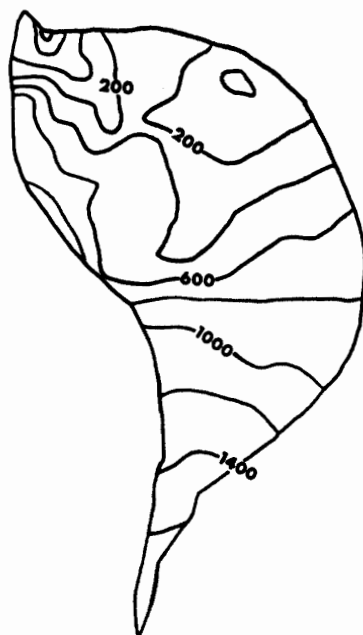


Fig. 3. Bedrock topography.

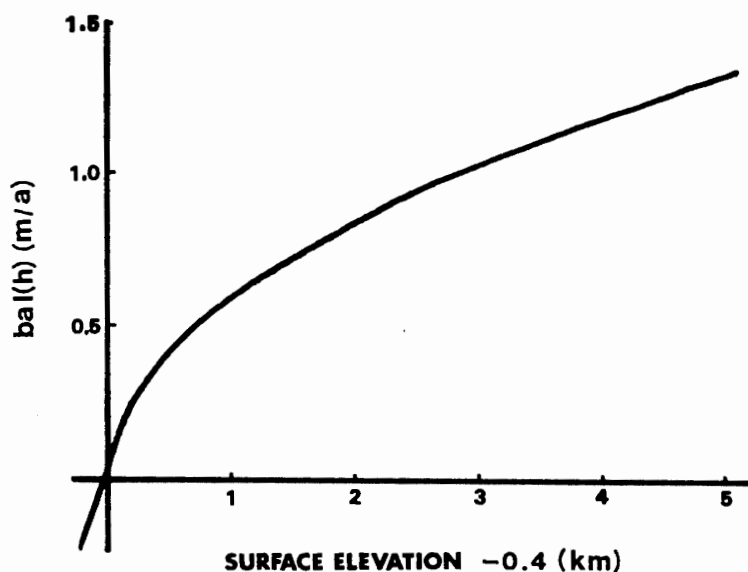


Fig. 4.  $bal(h)$  (m in water/a) as a function of the surface elevation of the ice sheet in eq. (3) (from NAGAO, 1982).

10 m snow temperatures compiled by SATOW (1978). In Mizuho Plateau the relation between 10 m snow temperature and elevation is expressed as temperature gradient with elevation. At elevation from 0 m to 1000 m, it is  $-0.8 \times 10^{-2}$  ( $^{\circ}\text{C}/\text{m}$ ). At elevation from 1000 m to 3000 m, it is  $-1.3 \times 10^{-2}$  ( $^{\circ}\text{C}/\text{m}$ ). And at higher elevation than 3000 m, it is  $-2.0 \times 10^{-2}$  ( $^{\circ}\text{C}/\text{m}$ ). For standard boundary condition in calculations, the temperature at sea level is chosen at  $-8$  ( $^{\circ}\text{C}$ ) to represent the present climate.

The geothermal heat flux ( $G$ ) of  $53 \text{ mW}/\text{m}^2$ ,  $55 \text{ mW}/\text{m}^2$  and  $57 \text{ mW}/\text{m}^2$  were used in the calculation. Since the geothermal heat flux is one of the major unknowns in the Antarctic ice sheet, the validity of these values are discussed later.

It should be noted that the accumulation rate in the up-stream region expressed by eq. (3) is about twice as large as that in the recent compilation of the surface mass balance (TAKAHASHI, private communication). Moreover, the field data of the bedrock elevation are still few in the up-stream region. Therefore the calculation in relation to the up-stream area is not necessarily reliable. So we mainly investigate and discuss the regions except the up-stream region.

#### 4. Numerical Experiments

The model was used to investigate the following questions concerning the ice sheet in the drainage basin. That is: (1) What is the equilibrium ice sheet profile which adjust to the present climate? (2) How the equilibrium state of ice sheet varies when boundary conditions, such as surface temperature, surface mass balance and geothermal heat flux, are changed? In order to investigate the above questions, seven preliminary numerical experiments were carried out with various boundary conditions. The present profile of the ice sheet was used as an initial profile of the ice sheet. The parameters tested in this study are surface temperature ( $T_s$ ), accumulation rate ( $A$ )

Table 1. Numerical experiments and parameters.

Experiment (No.)	Surface temperature ( $T_s$ )	Annual accumulation rate ( $A$ )	Geothermal heat flux ( $G$ ) (mW/m <sup>2</sup> )
1 standard experiment	present	$A_o$ (present value)	55
2	higher than present by 2°C	$A_o$	55
3	lower than present by 2°C	$A_o$	55
4	present	$0.8 \times A_o$	55
5	present	$1.2 \times A_o$	55
6	present	$A_o$	53
7	present	$A_o$	57

and geothermal heat flux ( $G$ ). The experiments and parameters are tabulated in Table 1. A numerical experiment using the present values of  $T_s$ ,  $A$  and  $G$  of 55 mW/m<sup>2</sup> is defined as the standard experiment.

## 5. Results

### 5.1. The standard experiment

Results of the calculations showed that an almost stationary state of the ice sheet was achieved after  $10^4$  model years when started from the present profile of the ice sheet. The time interval required for getting a computational stability is 50 years. When time interval is larger than 100 years, computations become unstable. The results of the standard experiment (No. 1) are shown in Figs. 5 and 6. Figure 5 shows computed surface elevation, bottom temperature, surface velocity and sliding velocity, of the ice sheet after  $10^4$  years. Figure 6 shows variation of the ice-thickness profile of a cross-section along the center flow line of the drainage basin with time. The equilibrium ice sheet profile shows that ice thickness decreases in the middle-stream region and increases in the down-stream region. In the experiments, fluctuation of the surface profile is relatively large in initial 500 years, then the profile gradually becomes stable, and reaches equilibrium by  $10^4$  years later.

### 5.2. Response to the change of the surface temperature

The results of experiments Nos. 2 and 3 are shown in Figs. 7, 8, 9 and 10. In the calculations,  $T_s$  higher by 2°C (experiment No. 2) and lower by 2°C (experiment No. 3) than their present values were used as the boundary conditions. Figure 7 shows the results of experiment No. 2. It shows (a) surface elevation, (b) bottom temperature, (c) surface velocity and (d) sliding velocity, of the ice sheet after  $10^4$  years. The bottom temperature (Fig. 7b) was higher than that of the standard experiment (Fig. 5b), and both surface and sliding velocity (Figs. 7c and d) was larger than those

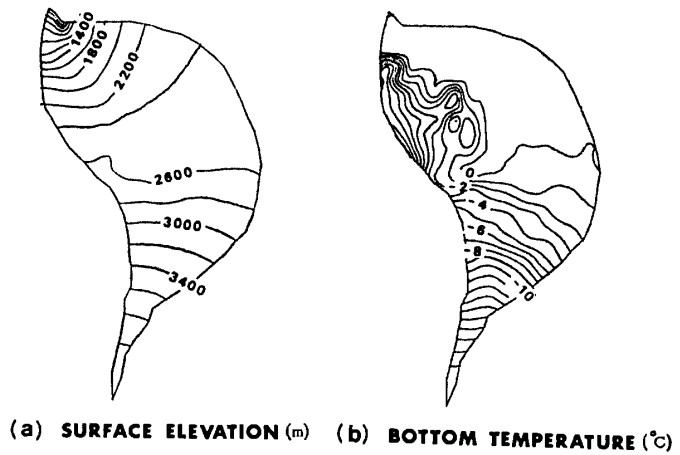


Fig. 5. The results of the experiment No. 1. The figures show the state of the ice sheet after  $10^4$  years. In the calculation, parameters of the present climate and the geothermal heat flux ( $G$ ) of  $55 \text{ mW/m}^2$  were used as the boundary condition.

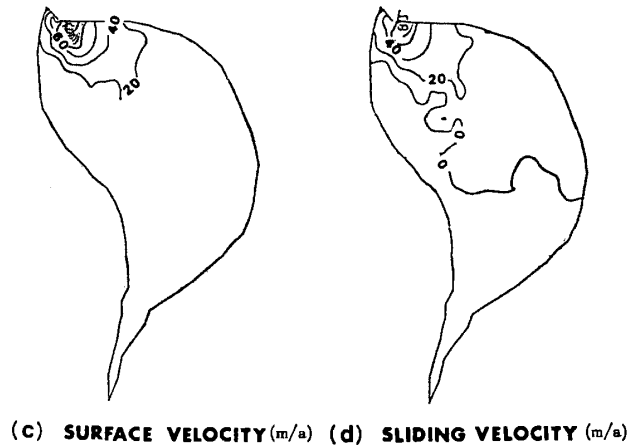
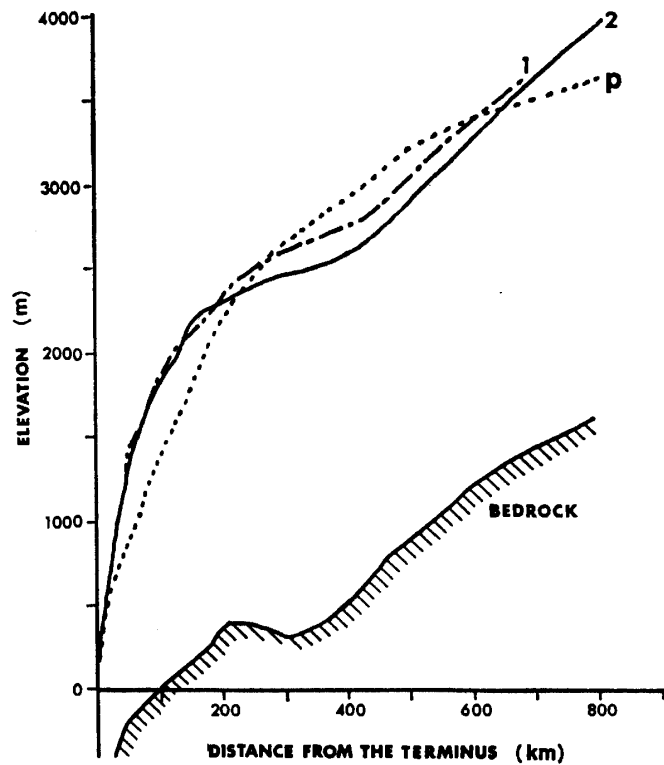


Fig. 6. Variations of the ice-thickness profile of a cross-section along the center flow line, with time, in experiment No. 1. The lines show the profiles of the ice sheet in following conditions, (p) present profile, (1) 2000 years later and (2)  $10^4$  years later.





of the standard experiment (Figs. 5c and d). The surface elevation in the middle-stream region (Fig. 7a) was lower than that of standard experiment (Fig. 5a).

Figure 8 shows the results of experiment No. 3. The bottom temperature (Fig. 8b) was lower than that of the standard experiment (Fig. 5b), and both surface and sliding velocity (Figs. 8c and d) were smaller than those of the standard experiment (Figs. 5c and d). The surface elevation of the middle-stream region (Fig. 8a) was higher than those of the standard experiment (Fig. 5a).

The ice-thickness profiles of a cross-section along the center flow line obtained from the experiment Nos. 2 and 3 are shown in Fig. 9. The difference in ice-thickness of the middle-stream area is about 100 m for difference in  $T_s$  by  $2^\circ\text{C}$ . The tendency that the elevation of the ice sheet becoming lower in the middle-stream region and higher in the down-stream region than that of the present ice sheet was similar to the standard experiment.

Figure 10 shows the ice-thickness profiles of cross-section along the westward boundary of the drainage basin obtained from the experiment Nos. 2 and 3. The ice sheet in the vicinity of the Yamato Mountains did not fluctuate compared to the

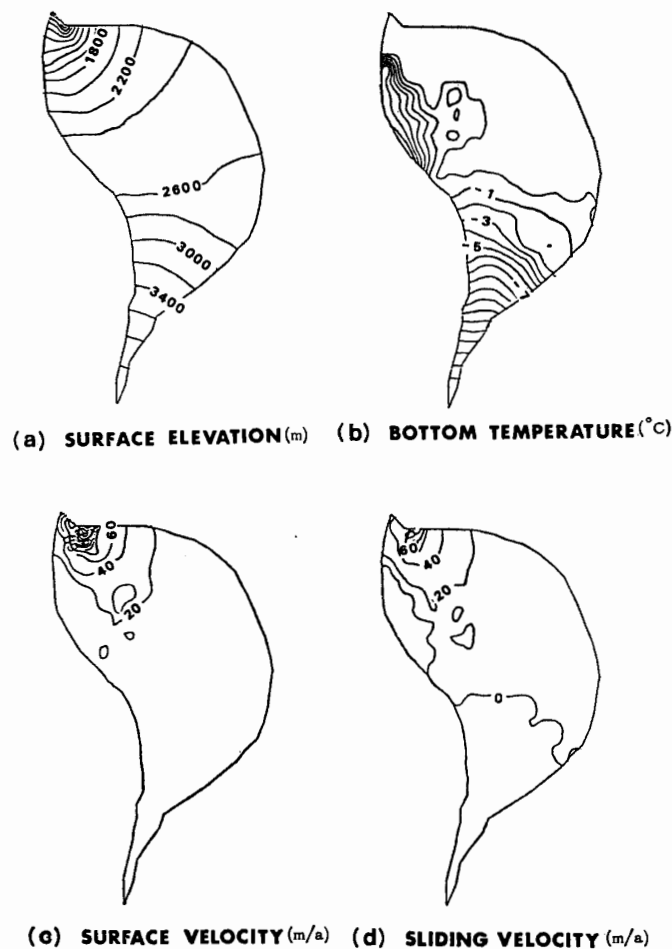


Fig. 7. The results of the experiment No. 2. The figures are same as Fig. 5 but for  $T_s$  higher than the present values by  $2^\circ\text{C}$ .

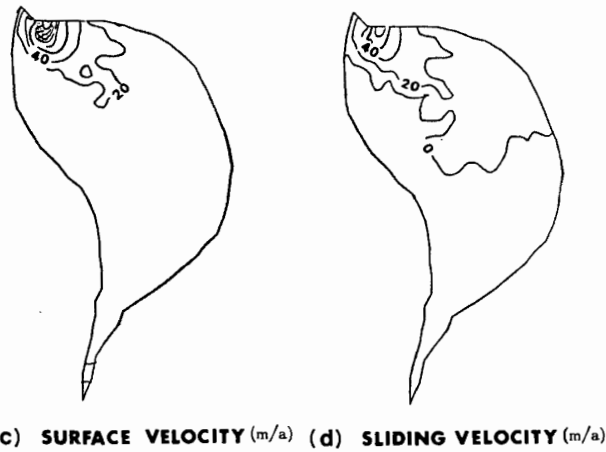
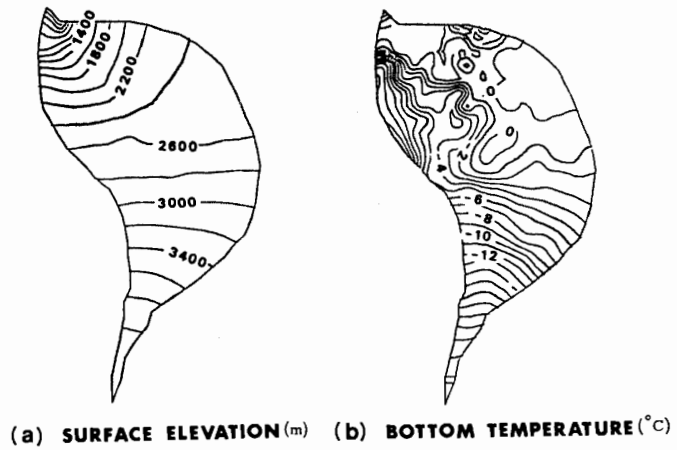


Fig. 8. The result of the experiment No. 3. The figures are same as Fig. 5 but for  $T_s$  lower than the present values by  $2^\circ\text{C}$ .

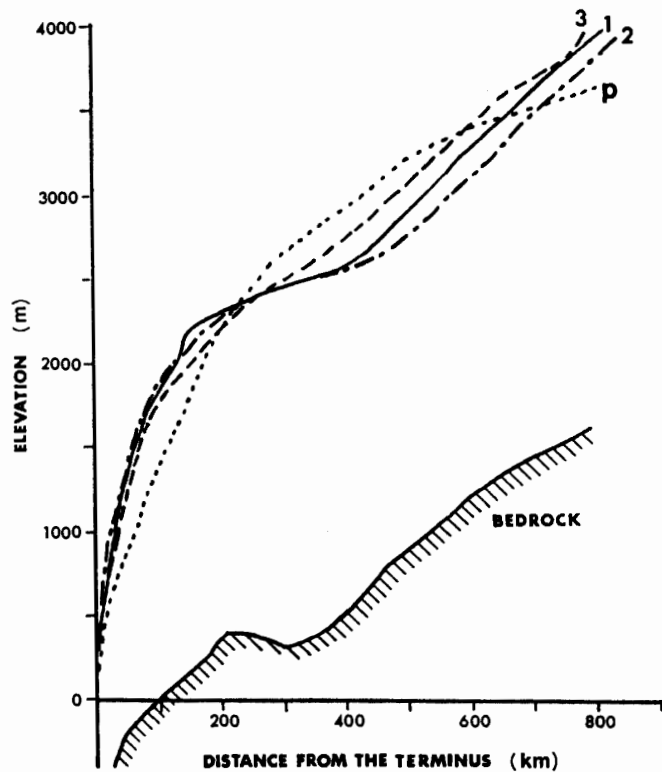


Fig. 9. The ice-thickness profiles of the ice-sheet after  $10^4$  years along the center flow line with various conditions  $T_s$ . The lines show the profiles of the ice sheet on following surface temperature conditions, (1) the present surface temperature condition (No. 1), (2)  $T_s$  higher by  $2^\circ\text{C}$  than present (No. 2) and (3)  $T_s$  lower by  $2^\circ\text{C}$  than present (No. 3). The present profile of the ice sheet is shown for comparison as the line p.

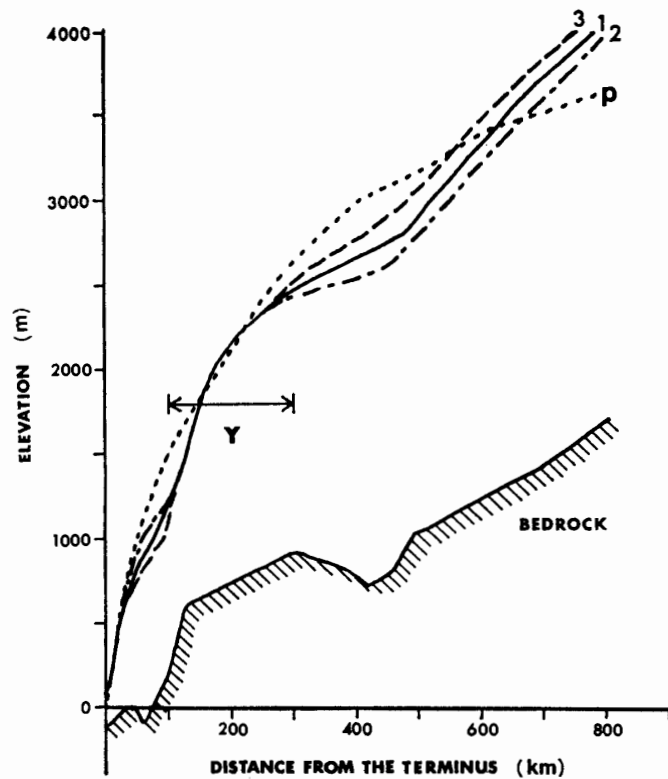


Fig. 10. The ice-thickness profiles of the ice sheet after  $10^4$  years along the flow line in the westward boundary of the drainage basin, with various condition of  $T_s$ . The region in the vicinity of the Yamato Mountains is denoted by "Y". The lines are same as Fig. 9.

profile along the center flow line (Fig. 9) even if  $T_s$  were changed. This tendency is discussed later.

### 5.3. Response to the change of annual accumulation rate

The results of the experiments No. 4 and 5 are shown in Figs. 11 and 12, respectively. In the calculations,  $A$  different from the present values were used as the boundary condition. Figures 11a and 11b show the surface elevation and the bottom temperature, respectively, of the equilibrium ice sheet after  $10^4$  years with  $A=0.8A_0$ . Here  $A_0$  means the present values of accumulation rate. Figures 11c and 11d show the surface elevation and the bottom temperature, respectively, of equilibrium ice sheet after  $10^4$  years with  $A=0.8A_0$ . Figure 12 shows the ice-thickness profiles of a cross-section along the center flow line.

With  $A=1.2A_0$ , the computed bottom temperatures (Fig. 11b) became higher than those of the standard experiment (Fig. 5b), and the surface elevation (Fig. 11a) and the line "2" in Fig. 12) became lower than that of the standard experiment (Fig. 5a and the line "1" in Fig. 12). With  $A=0.8A_0$ , the bottom temperatures (Fig. 11d) became lower than those of the standard experiment (Fig. 5b), and the surface elevation (Fig. 11c and the line "3" in Fig. 12) became higher than that of the standard experiment (Fig. 5a and the line "1" in Fig. 12).

The surface elevation in the middle-stream region of the ice sheet became lower

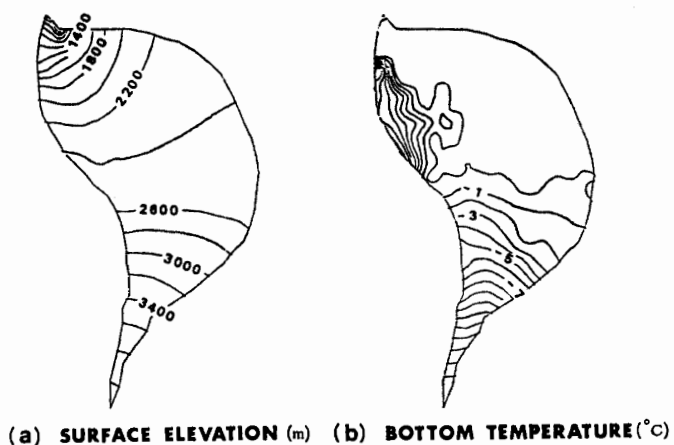


Fig. 11. The results of the experiments Nos. 4 and 5. In the calculations, accumulation rate  $A=0.8 A_0$  (a, b; No. 4) and  $A=1.2 A_0$  (c, d; No. 5) ( $A_0$  is the present values) were used as the boundary conditions.

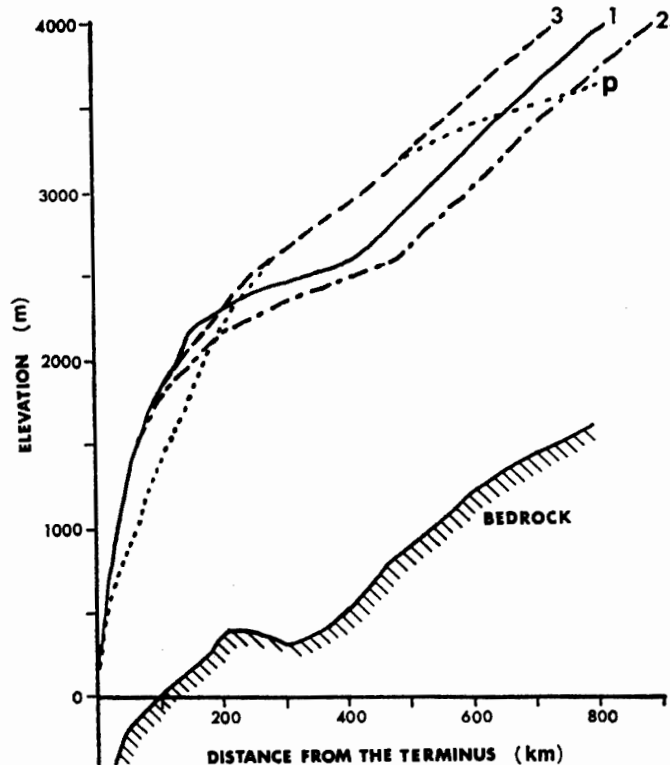
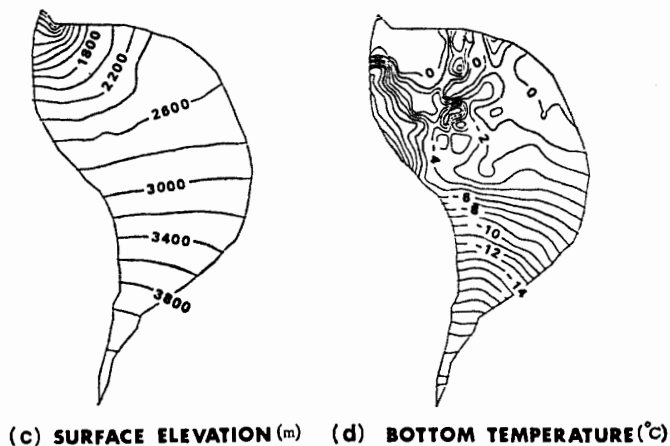


Fig. 12. The ice-thickness profiles are same as Fig. 9 but for accumulation rate. The lines show the profile of the ice sheet, (1) with  $A=A_0$  (No. 1), (2) with  $A=0.8 A_0$  (No. 5) and (3) with  $A=1.2 A_0$  (No. 4).

than that of the present ice sheet with  $A=0.8A_0$ . However, it became almost the same as that of the present ice sheet with  $A=1.2A_0$ .

#### 5.4. Response to the geothermal heat flux

The results of the experiments Nos. 6 and 7 are shown in Figs. 13 and 14. In the calculations,  $G$  of  $53 \text{ mW/m}^2$  and  $57 \text{ mW/m}^2$  were used as the boundary conditions. Figures 13a and 13b show the surface elevation and the bottom temperatures, respectively, of the equilibrium ice sheet after  $10^4$  years with  $G$  of  $53 \text{ mW/m}^2$ . Figures 13c and 13d show the surface elevation and the bottom temperature, respectively, of the equilibrium ice sheet after  $10^4$  years with  $G$  of  $57 \text{ mW/m}^2$ . Figure 14 shows the ice-thickness profiles of a cross-section along the center flow line.

With  $G$  of  $53 \text{ mW/m}^2$ , the bottom temperatures (Fig. 13b) became lower than those of the standard experiment (Fig. 5b), and the surface elevation (Fig. 13a and the line "3" in Fig. 14) became higher than that of the standard experiment (Fig. 5a and the line "1" in Fig. 14). With  $G$  of  $57 \text{ mW/m}^2$ , the bottom temperatures (Fig. 13d) became higher than those of the standard experiment (Fig. 5b), and the surface elevation (Fig. 13c and the line "2" in Fig. 14) became lower than that of the standard

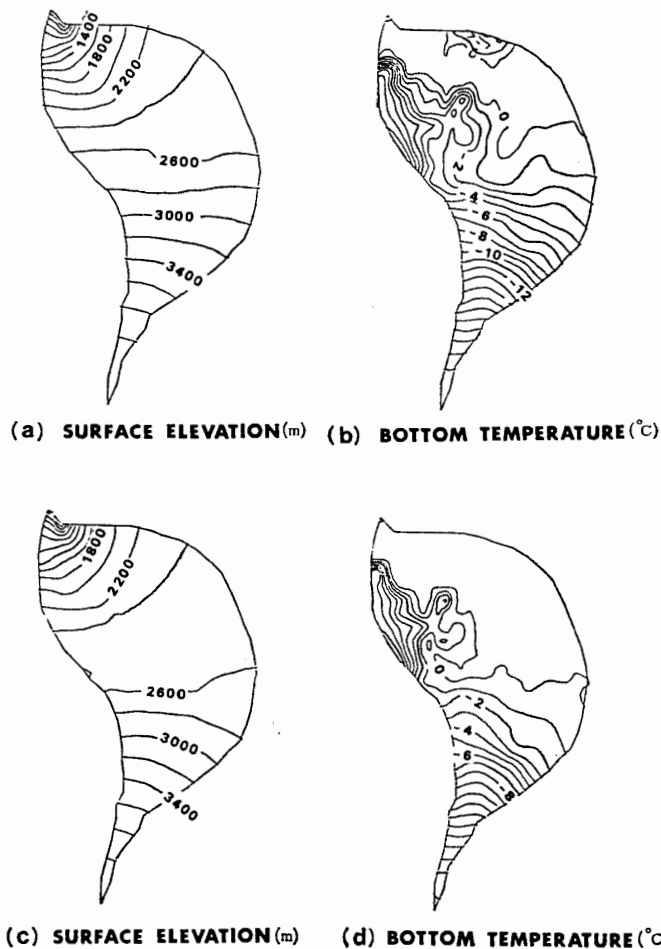


Fig. 13. The results of the experiments Nos. 6 and 7. In calculations,  $G$  of  $53 \text{ mW/m}^2$  (a, b; No. 6) and  $57 \text{ mW/m}^2$  (c, d; No. 7) were used as the boundary conditions.

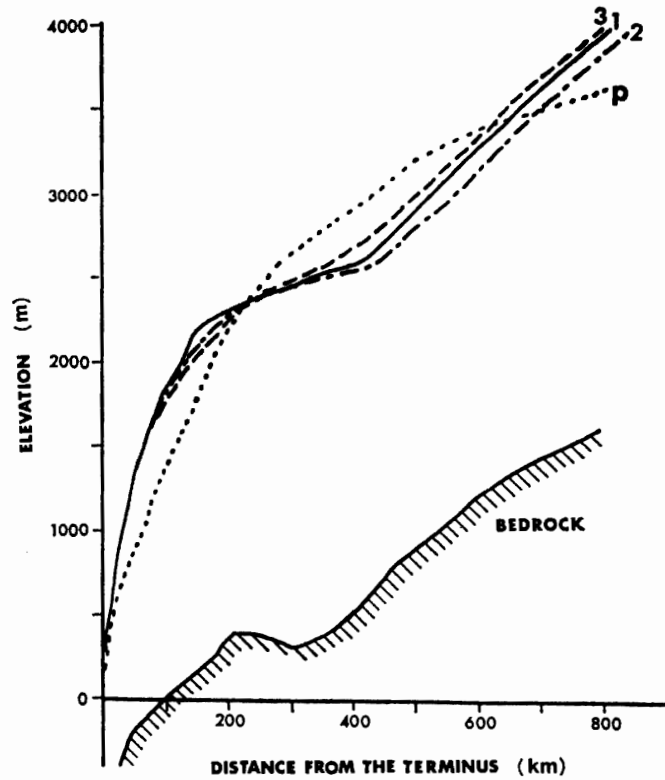


Fig. 14. The ice-thickness profiles of the ice sheet after  $10^4$  years along the center flow line with various conditions of  $G$ . The lines show the profiles of the ice sheet, (1)  $G=55 \text{ mW/m}^2$  (No. 1), (2)  $G=57 \text{ mW/m}^2$  (No. 7) and (3)  $G=53 \text{ mW/m}^2$  (No. 6). The line  $p$  is same as Fig. 9.

Table 2. Results of the experiments (comparison with the standard experiment).

Experiment (No.)	Surface elevation in the middle-stream region (higher: $\uparrow$ ; lower: $\downarrow$ )	Bottom temperature	Surface velocity (larger: $\uparrow$ ; smaller: $\downarrow$ )	Sliding velocity
2	$\downarrow$	$\uparrow$	$\uparrow$	$\uparrow$
3	$\uparrow$	$\downarrow$	$\downarrow$	$\downarrow$
4	$\downarrow$	$\uparrow$	$\uparrow$	$\uparrow$
5	$\uparrow$	$\downarrow$	$\downarrow$	$\downarrow$
6	$\uparrow$	$\downarrow$	$\downarrow$	$\downarrow$
7	$\downarrow$	$\uparrow$	$\uparrow$	$\uparrow$

experiment (Fig. 5a and the line "1" in Fig. 14). The tendency that the surface elevation of the ice sheet become lower in the middle-stream region and higher in the down-stream region than that of the present ice sheet was similar to the results of the standard experiment. The results of experiments No. 2 to No. 7 are compared with those of No. 1 in Table 2.

## 6. Discussion

### 6.1. The surface elevation of the ice sheet and the parameters

The surface elevation in the middle-stream region of the equilibrium ice sheet becomes lower than that of the standard experiment by (a) increasing  $T_s$  by  $2^\circ\text{C}$  compared to their present values (experiment No. 2), or (b) reducing  $A$  to 80% of

their present values (experiment No. 4), or (c) using  $G$  of  $57 \text{ mW/m}^2$  (experiment No. 7). On the contrary, it becomes lower than that of the standard experiment by (a) reducing  $T_s$  by  $2^\circ\text{C}$  compared to their present values (experiment No. 3), or (b) increasing  $A$  to 120% of the present values (experiment No. 5), or (c) using  $G$  of  $53 \text{ mW/m}^2$  (experiment No. 6). As shown in Table 2, the surface elevation becomes lower when the bottom temperature is higher while it becomes higher when the bottom temperature is lower.

The relation between the surface elevation and the bottom temperature can be interpreted as follows. The higher bottom temperature enhances the flow of the ice sheet because an amount part of the shear deformation occurs near the bottom and the deformation rate of ice increases exponentially with temperature. Moreover, the higher temperature at the bottom widens the area in which the bottom is at the pressure melting point and thus the area of basal sliding. As a result, a larger amount of the ice mass flows away from the middle-stream region and the surface elevation in the middle-stream region becomes lower. On the contrary, the lower bottom temperature reduces the flow of the ice sheet. Because, the lower temperature at the bottom reduces both the deformation rate of ice and the area in which the bottom is at the pressure melting point and thus the area of basal sliding. As a result, a smaller amount of the ice mass flows from the middle-stream region and the surface elevation in the middle-stream region becomes relatively higher.

### 6.2. *The equilibrium profile of the ice sheet*

All of the results of the experiments except No. 5 revealed that the surface elevation of the middle-stream region became lower than that of the present ice sheet. The results suggest that the present ice sheet may tend to decrease its thickness in the middle-stream region to adjust the present climate.

The difference of the surface elevation from that of the present in the middle-stream region is larger when the bottom temperature is higher (*e.g.* experiment Nos. 2, 4 and 7), and smaller when the bottom temperature is lower (*e.g.* experiment Nos. 3, 5 and 6). Thus the profile of the ice sheet become closer to that of the present ice sheet when the basal sliding mechanism and enhancement of the shear deformation near the bottom are less effective. Therefore, the results of the experiment suggest that the basal sliding and deformation of ice near the bottom determine the equilibrium profile of the ice sheet. From this point of view, the increase of the area of basal sliding and the activation of deformation rate can be one explanation for recent thinning of the ice sheet, as proposed by MAE and NARUSE (1978) and NISHIO *et al.* (1989).

Here the calculated results are compared with the observations. The area with high value of reflection intensity of radio echo is the area where the present surface elevation is lower than about 2500 m (OHMAE *et al.*, 1989). This area roughly corresponds to the area where the bottom is at the melting point in the results of the present study (Fig. 5b). Moreover, this area roughly corresponds to the area of thinning ice sheet observed by NARUSE (1978, 1979) and NISHIO *et al.* (1989).

The model, however, suggested that the ice sheet in the region where the surface elevation is lower than about 2300 m finally thickens. Since the ice sheet profile in the down-stream region may be affected by constrained boundary conditions of the model, this tendency should be further investigated with the numerical model which

involves proper seaward boundary condition and effect of longitudinal stress. The possibility that the ice sheet in the down-stream region thickens was mentioned by MAE (1979). According to estimation based on observations, the mass balance of the Shirase Glacier drainage basin is positive (SHIMIZU *et al.*, 1978), whereas the ice sheet is thinning in Mizuho Plateau. MAE (1979) suggested if estimation of total accumulation is correct, the positive mass balance in the drainage basin indicates that a thickening may take place down-glacier. The observation showed, however, that the ice sheet is thinning even at the G2 station (71°02'25''S, 39°51'47''E) where surface elevation is 1787 m (NISHIO *et al.*, 1989). The thickness changes in down-glacier where the surface elevation is lower than G2 station have not been reported so far. It should be examined whether thickening is taking place there.

### 6.3. *The effect of the bedrock topography and the stability of the ice sheet in the vicinity of the Yamato Mountains*

As shown in the results of the experiments (Figs. 5, 7, 8, 11 and 13), bottom temperature, surface velocity, sliding velocity and thus the equilibrium ice sheet profile, depend on the bedrock topography (Fig. 3). The results of the experiments showed that the bottom temperature was higher in the area in which the bedrock elevation was lower, and thus the amount of mass flux become larger. On the contrary, bottom temperature was lower in the area in which the bedrock elevation was higher, and thus the amount of mass flux became smaller. Moreover, the flow of the ice sheet tend to be more stagnant there because thickness of the ice sheet is relatively thin. Such different aspect of the ice flow between areas where surface elevation is high and low clearly can be seen in the ice sheet near the Yamato Mountains and the eastern side of the drainage basin (Figs. 5, 7, 8, 11 and 13).

Figure 10 also shows that fluctuation of the ice sheet was small in the vicinity of the Yamato Mountains even if  $T_s$  were changed. Moreover, it was stable not only in the experiment in which surface temperature was changed but also in the other results of the experiments although they were not shown like Fig. 10 in this paper. The tendency that the ice sheet there is relatively stable is due to the higher bedrock elevation than that of the other region. This result suggest that the ice sheet there is stable in the period of time of the order of  $10^4$  years if it is assumed that the ice sheet outside the western boundary of the drainage basin do not change significantly during then.

### 6.4. *The geothermal heat flux*

BUDD and JENSSEN (1989) showed that basal temperatures were closely dependent on the geothermal heat flux in a three-dimensional model of the whole Antarctic ice sheet. According to them, the geothermal heat flux  $51.7 \text{ mW/m}^2$  fits closely to the observed deep temperature profile in the drill-hole at Vostok. This estimation can be supported by the interpretation of temperature profile at Vostok Station by RITZ (1989) that the geothermal heat has to be higher than  $50 \text{ mW/m}^2$ . In the present study the geothermal heat flux lower than  $53 \text{ mW/m}^2$  seems to make the calculated ice sheet profile closer to the present one (Fig. 14).

The geothermal heat flux and its distribution still remain unknown in the Antarctic ice sheet, and it should be further studied by analyzing observed temperature profiles in drill-holes in the studied area.



### Acknowledgments

The authors wish to thank Dr. H. OHMAE (Space Division, Fujitsu Limited) for making compiled bedrock topography map available to this study. The authors also wish to thank Dr. M. NISHIMURA (Chief Researcher of Research Institute of Computer Science (SRICS), Sapporo) for helpful advice and suggestions on computations. Computations were carried out on computer language "DEQSOL" on HITAC S-810-10 at Hokkaido University Computing Center. This study is a contribution from the Glaciological Research Program in East Queen Maud Land by Japanese Antarctic Research Expedition.

### References

- AGETA, Y., KIKUCHI, T., KAMIYAMA, K. and OKUHIRA, F. (1987): Position, elevation and ice thickness of the stations. *JARE Data Rep.*, **125** (Glaciology 14), 5-29.
- BUDD, W. F. and JENSSSEN, D. (1989): The dynamics of the Antarctic ice sheet. *Ann. Glaciol.*, **12**, 16-22.
- FUJII, Y., KAWADA, K., YOSHIDA, M. and MATSUMOTO, M. (1986): Position, elevation and ice thickness of the stations. *JARE Data Rep.*, **116** (Glaciology 13), 5-27.
- MAE, S. (1979): The basal sliding of a thinning ice sheet, Mizuho Plateau, East Antarctica. *Glaciol.*, **24**, 53-61.
- MAE, S. and NARUSE, R. (1978): Possible causes of ice sheet thinning in the Mizuho Plateau. *Nature*, **273**, 291-292.
- MAE, S. and YOSHIDA, M. (1987): Airborne radio echo-sounding in Shirase Glacier drainage basin, Antarctica. *Ann. Glaciol.*, **9**, 160-165.
- MAHAFFY, M. W. (1976): A three-dimensional numerical model of ice sheets: Test on the Barnes Ice Cap, Northwest Territories. *J. Geophys. Res.*, **81**, 1059-1066.
- NAGAO, M. (1982): Nankyoku Shirase Hyôga ryûiki no keisanki simyurêshon (Computer simulation of the ice flow in the Shirase Glacier drainage basin, Antarctica). Master thesis, Hokkaido University.
- NAGAO, M., NAKAWO, M. and HIGASHI, A. (1982): A simple method for calculation mass flux in an ice sheet, with a consideration of its temperature profile. *Mem. Natl. Inst. Polar Res., Spec. Issue*, **24**, 192-200.
- NAGAO, M., NAKAWO, M. and HIGASHI, A. (1984): Computer simulation of the ice sheet in the Shirase basin, Antarctica (abstract). *Ann. Glaciol.*, **5**, 219-221.
- NARUSE, R. (1978): Surface flow and strain of the ice sheet measured by a triangulation chain in Mizuho Plateau. *Mem. Natl. Inst. Polar Res., Spec. Issue*, **7**, 198-226.
- NARUSE, R. (1979): Thinning of ice sheet in Mizuho Plateau, East Antarctica. *J. Glaciol.*, **24**(90), 45-52.
- NISHIO, F., ISHIKAWA, M. and OHMAE, H. (1984): Position, elevation and ice thickness of the stations between Syowa Station and Mizuho Station. *JARE Data Rep.*, **94** (Glaciology 10), 6-14.
- NISHIO, F., OHMAE, H. and ISHIKAWA, M. (1986): Position, elevation and ice thickness of the stations. *JARE Data Rep.*, **110** (Glaciology 12), 5-36.
- NISHIO, F., MAE, S., OHMAE, H., TAKAHASHI, H., NAKAWO, M. and KAWADA, K. (1989): Dynamical behavior of the ice sheet in Mizuho Plateau, East Antarctica. *Proc. NIPR Symp. Polar Meteorol. Glaciol.*, **2**, 97-104.
- OHMAE, H., NISHIO, F. and MAE, S. (1989): Distribution of reflected power from the bed by radio echo-sounding in the Shirase Glacier drainage area, East Queen Maud Land, Antarctica. *Ann. Glaciol.*, **12**, 124-126.
- RADOK, U., JENSSSEN, D. and BUDD, W. F. (1970): Steady-state temperature profiles in ice sheets. *International Symposium on Antarctic Glaciological Exploration (ISAGE)*, ed. by A. J. Gow *et al.* Cambridge, SCAR, 151-165 (Publ. No. 86).

- RITZ, C. (1989): Interpretation of the temperature profile measured at Vostok, East Antarctica. *Ann. Glaciol.*, **12**, 138–144.
- SATOW, K. (1978): Distribution of 10 m snow temperatures in Mizuho Plateau. *Mem. Natl Inst. Polar Res., Spec. Issue*, **7**, 63–71.
- SHIMIZU, H., WATANABE, O., KOBAYASHI, S., YAMADA, T., NARUSE, R. and AGETA, Y. (1978): Glaciological aspects and mass budget of the ice sheet in Mizuho Plateau. *Mem. Natl Inst. Polar Res., Spec. Issue*, **7**, 264–274.
- YAMADA, T. and WATANABE, O. (1978): Estimation of mass input in the Shirase and the Sôya drainage basins in Mizuho Plateau. *Mem. Natl Inst. Polar Res., Spec. Issue*, **7**, 182–197.
- WEETMAN, J. (1957): On the sliding of glaciers. *J. Glaciol.*, **3**, 33–38.

*(Received December 12, 1990; Revised manuscript received February 8, 1991)*